Associations between ADHD symptom remission and white matter microstructure: a longitudinal analysis

A.E.M.Leenders[1*], C.G.Damatac[1,2*], S.Soheili-Nezhad[1,2], R.J.M.Chauvin[1,2], M.J.J.Mennes[1,2], M.P.Zwiers[1,2], D.vanRooij[1,2], S.E.A.Akkermans[1,3], J.Naaijen[1,2], B.Franke[3,4], J.K.Buitelaar[1,2,5], C.F.Beckmann[1,2,6], E.Sprooten[1,2]

[1]Centre for Cognitive Neuroimaging, Donders Institute for Brain, Cognition and Behaviour, Radboud University, Nijmegen, the Netherlands; [2]Department of Cognitive Neuroscience, Donders Institute for Brain, Cognition and Behaviour, Radboud University Medical Centre, Nijmegen, the Netherlands; [3]Department of Human Genetics, Donders Institute for Brain, Cognition and Behaviour, Radboud University Medical Centre, Nijmegen, the Netherlands; [4]Department of Psychiatry, Donders Institute for Brain, Cognition and Behaviour, Radboud University, Nijmegen, the Netherlands; [5]Karakter Child and Adolescent Psychiatry University Centre, Nijmegen, the Netherlands; [6]Centre for Functional MRI of the Brain, University of Oxford, Oxford, UK

* Authors contributed equally to this work.

Abstract

Background: Attention-deficit hyperactivity disorder (ADHD) is associated with white matter (WM) microstructure. Our objective was to investigate how WM microstructure is longitudinally related to symptom remission in adolescents and young adults with ADHD. **Methods:** We obtained diffusion-weighted imaging (DWI) data from 99 participants at two time points (mean age baseline: 16.91 years, mean age follow-up: 20.57 years). We used voxel-wise Tract-Based Spatial Statistics (TBSS) with permutation-based inference to investigate associations of inattention (IA) and hyperactivity-impulsivity (HI) symptom change with fractional anisotropy (FA) at baseline, follow-up, and change between time points. **Results:** Remission of combined HI and IA symptoms was significantly associated with reduced FA at follow-up in the left superior longitudinal fasciculus and the left corticospinal tract (CST) (P_{FWE}=0.038 and P_{FWE}=0.044, respectively), mainly driven by an association between HI remission and follow-up CST FA (P_{FWE}=0.049). There was no significant association of combined symptom decrease with FA at baseline or with changes in FA between the two assessments. **Conclusions:** In this longitudinal DWI study of ADHD using dimensional symptom scores, we show that greater symptom decrease is associated with lower follow-up FA in specific WM tracts. Altered FA thus may appear to follow, rather than precede, changes in symptom remission. Our findings indicate divergent WM developmental trajectories between individuals with persistent and remittent ADHD, and support the role of prefrontal and sensorimotor tracts in the remission of ADHD.

Keywords: ADHD; white matter; dMRI; remission; longitudinal. **Abbreviations:** white matter(WM), NeuroIMAGE1(TP1), NeuroIMAGE2(TP2)

Introduction

Attention-deficit/hyperactivity disorder (ADHD) is a common neuropsychiatric disorder characterized by developmentally inappropriate levels of inattention (IA) and/or hyperactivity-impulsivity (HI), with an estimated prevalence of 5% in children and adolescents and 2.5% in adults(Faraone et al., 2015). For many, ADHD begins in childhood, but the long-term clinical course of ADHD varies widely between individuals(American Psychiatric Association, 2013). Prospective studies suggest that although only 15% of children with ADHD continue to fully meet diagnostic criteria in adulthood, 60-70% of them retain impairing symptoms in adulthood(Faraone et al., 2015). ADHD diagnosis has been associated with altered patterns of brain structure and function, however the neural mechanisms related to symptom progression (i.e. remission vs. persistence) have not yet been fully unraveled (Aoki, Cortese, & Castellanos, 2018; Damatac et al., 2020; Francx, Zwiers, et al., 2015; Franke et al., 2018; Hoogman et al., 2017). Understanding this could help develop and tailor treatments to benefit long-term outcomes for children with ADHD.

The underlying neural mechanisms that drive symptom remission may be distinct from those that drive ADHD onset, thus the brains of remitted individuals could be methodologically differentiated from those of people who were never diagnosed with ADHD(Halperin & Schulz, 2006). Here, we refer to symptom remission as a dimensional concept, as a decrease in symptom severity between two time-points. Symptom remission can be driven by a number of neurodevelopmental mechanisms which are not mutually exclusive. Previous hypotheses suggest that disorder onset is characterized by a fixed anomaly or ‘scar’, while symptom remission or persistence is associated with brain maturation and normalization, or compensation and reorganization(Sudre, Mangalmurti, & Shaw, 2018). The trajectories of remission and persistence from childhood through adulthood occur in parallel to or in interaction with other neurodevelopmental processes (e.g.development of executive functions).

The development of frontal and temporal areas engaged in emotional and cognitive processes does not plateau until adulthood, which coincides with the typical age range of ADHD symptom remission(Faraone et al., 2015; Lebel & Deoni, 2018). Maturation in these regions may compensate for the initial childhood development of ADHD symptoms through top-down regulatory processes, leading to eventual symptom remission(Halperin & Schulz, 2006). Therefore, longitudinal cohort studies are essential to dissect the upstream, parallel, or downstream brain mechanisms in reference to symptom remission. Compared to a cross-sectional approach, a longitudinal design provides not only unique insights into the temporal dynamics of underlying biological processes, but also increased statistical power by reducing between-subject variability(Madhyastha et al., 2014).

Neurodevelopmental mechanisms underlying the variable long-term course of ADHD may be partly traceable using neuroimaging. Healthy brain development has been characterized using structural and functional magnetic resonance imaging (MRI), showing trajectories across the lifespan of regional volumes and activity/connectivity, respectively(Brouwer et al., 2020; van Duijvenvoorde, Westhoff, de Vos, Wierenga, & Crone, 2019). Those that have applied diffusion, magnetization transfer, relaxometry, and myelin water imaging methods have also demonstrated consistent, rapid white matter (WM) microstructural changes in the first three years of life, reflecting increased myelination or axonal packing(Lebel & Deoni, 2018). These changes continue throughout adolescence and are associated with corresponding age-related changes in gray matter(Giorgio et al., 2008). However, regarding later childhood and adolescence, the paucity of congruous findings in other WM imaging modalities besides diffusion weighted imaging (DWI) suggests that changes are primarily related to myelination and axonal packing(Lebel & Deoni, 2018). With age, WM increases in overall volume, becoming more myelinated in a region-specific fashion and reaching peak values later in life(Kochunov et al., 2012; Paus et al., 2001). The rate of development differs between WM

regions, progressing in an outward, central-to-peripheral direction, wherein sensory and motor regions generally mature the earliest.

DWI studies have revealed WM microstructural abnormalities in ADHD, specifically using fractional anisotropy (FA), which is the metric we focus on here(Aoki et al., 2018; Damatac et al., 2020; van Ewijk et al., 2014; Francx, Oldehinkel, et al., 2015; Shaw et al., 2015; Sudre et al., 2018). DWI reveals information about anatomical connectivity in the brain *in vivo* by measuring the directionality of water diffusion in WM tracts, thus enabling inferences about underlying brain mechanisms by quantifying associated changes in (inter)cellular space(Beaulieu, 2002; van Ewijk et al., 2014). FA is an indirect measure of microstructural integrity—sensitive to myelination, parallel organization and fiber bundle density. A systematic meta-analysis of case-control DWI studies in ADHD found that lower FA in ADHD has mostly been reported in interhemispheric, frontal and temporal regions—however, higher FA has also been found in similar areas(Aoki et al., 2018). Given these previous WM associations with ADHD and the brain's maturation in those same areas during an age range typical for symptom remission, the next step is to determine how WM microstructural alterations coincide with remission versus persistence of ADHD symptoms over time.

Not many longitudinal studies have examined the neurobiological underpinnings of symptom remission in WM—and none have longitudinally applied DWI. While there are no previous studies with longitudinal DWI measurements, there have been some clinical longitudinal studies with one DWI measurement. A follow-up DWI analysis three decades after diagnosis supports the theory of the disorder as an enduring neurobiological trait independent of remission; both remittent and persistent probands with an ADHD diagnosis in childhood had widespread reduced FA compared to those who did not have childhood ADHD(Cortese et al., 2013). Conversely, a network connectivity analysis of two clinical assessments and one

resting-state functional MRI measurement at follow-up pointed to the presence of compensatory mechanisms that aid symptomatic remission in prefrontal regions and the executive control network: higher connectivity at follow-up was associated with HI decreases (Francx, Oldehinkel, et al., 2015). A study performed with a sample overlapping with the current study (but at an earlier sampling time with mean age 11.9-17.8 years) found, somewhat counterintuitively, that more HI symptom remission was associated with lower FA in the left corticospinal tract (lCST) and left superior longitudinal fasciculus (lSLF) at follow-up(Francx, Zwiers, et al., 2015). This previous study included clinical data from two time-points and only one DWI time-point.

Our current investigation is a continuation of our earlier DWI work in this cohort, and extends upon it in three ways. First, by capturing an older age range, we have a more complete picture of symptom remission (mean age range: 16.91-20.57 years; Figure 1 illustrates how our study chronologically relates to that of Francx *et al.*(2015). Second, DWI measurements at two time-points allow for a more thorough investigation of the chronology and mechanisms of FA development in relation to symptom remission. Third, we used Permutation Analysis of Linear Models(PALM), a newly available permutation-based analysis technique, to account for the family structure in our sample(Winkler, Webster, Vidaurre, Nichols, & Smith, 2015). We aimed to examine whether symptom remission may be underpinned by WM alterations as adolescents with ADHD develop into adulthood. Given our longitudinal DWI data, we were able to distinguish between (1) pre-existing WM features that predict the likelihood of symptoms to remit or persist, (2) WM changes over time that occur concurrently with symptom change, and (3) WM alterations that may be a (direct or indirect) downstream consequence of symptom remission versus persistence.

141 **Methods**

142 *Participants*

143 Clinical and MRI data were collected in two waves from probands with childhood ADHD,
144 their first-degree relatives, and healthy families: NeuroIMAGE1(TP1) and
145 NeuroIMAGE2(TP2)(Müller et al., 2011a, 2011b; von Rhein et al., 2015). The current study
146 included probands, affected and unaffected siblings, and healthy controls who participated in
147 both TP1 and TP2 and had DWI data from both waves(N=120). After we excluded
148 subjects(Figure S1), there were 99 participants from 65 families in our final sample (see
149 characteristics in Table 1). For both time-point groups, there were no differences between the
150 participants included in the current analysis and the complete sample on measures of ADHD
151 severity, age, and sex(P>0.05). We normalized head motion z-scores after excluding outliers.
152 Global FA at TP1, TP2, and the difference between TP1 and TP2 were normally distributed.

153 Given the longitudinal design of our study, we did not split our participants into cases
154 versus controls; there were those who were diagnosed as unaffected at both time-points, as well
155 as those who had a symptom score of zero in all dimensions at both time-points (Figure S2).
156 Our sample includes controls, or people who do not have (subthreshold) ADHD; however, this
157 group of people changed between the waves of the study (Figure S3). Some individuals
158 originally recruited as controls or unaffected siblings developed ADHD at a later time point
159 and others recruited as patients remitted. Moreover, ADHD may be operationalized as a
160 continuous trait rather than a binary diagnostic variable, especially in longitudinal studies
161 (Lahey & Willcutt, 2010; Marcus & Barry, 2011). In a previous cross-sectional study we
162 specifically showed that, compared to categorical diagnoses, continuous symptom measures
163 were more sensitive to diffusion-weighted brain features in this sample (Damatac et al., 2020).
164 Therefore, we focus on participants' ADHD symptom scores in all models, thus optimizing our

design and methods for capturing the dynamic and continuous nature of the ADHD spectrum throughout adolescence.

Clinical measurements

Conners Parent Rating Scale(CPRS) questionnaires were used to assess the severity of 27 inattention(IA) and hyperactive-impulsive(HI) symptoms at TP1 and TP2(Conners et al., 1999). We used CPRS instead of the self-rated report because it was the consistent measure across waves and ages. We used raw CPRS scores to increase the distribution width, and analyzed HI, IA, and combined symptom scores per subject, per time-point. Here, we define symptom change as the score difference:$\Delta CPRS = CPRS_{TP1} - CPRS_{TP2}$. Thus, a more positive Δ value indicates more symptom improvement.

Data acquisition and DWI pre-processing

MRI data were acquired with a 1.5-Tesla AVANTO scanner(Siemens, Erlangen, Germany). The scanner was equipped with an 8-channel receive-only phased-array head coil. Whole-brain diffusion-weighted images were collected(twice refocused pulsed-gradient spin-echo EPI; 60 diffusion-weighted directions spanning an entire sphere; b-value 1000s/mm^2; 5 non-diffusion weighted images; interleaved slice acquisition; TE/TR=97/8500ms; GRAPPA-acceleration factor 2; no partial Fourier; voxel size 2x2x2.2mm). DWI acquisition parameters are described in detail elsewhere(von Rhein et al., 2015).

Longitudinal TBSS

We performed whole brain voxel-wise analyses with Tract-Based Spatial Statistics (TBSS)(Smith et al., 2006). Our study's longitudinal design necessitated an analysis pipeline that considered how within-subject changes may be greater than between-subject changes; intra-subject data alignment across time brings extra difficulty compared to cross-subject nonlinear registration to common space. We used a bespoke pipeline adapted from others to

create non-biased individual subject templates(Madhyastha et al., 2014). Figure 2 summarizes our pipeline(detailed in Figure S1).

Statistical analysis

We constructed three general linear models for our voxel-wise analyses (Table S1). We kept difference in raw CPRS score(ΔCPRS) as a constant predictor, while separately testing FA at baseline(FA_{TP1}), follow-up(FA_{TP2}), and the difference between TP1 and TP2 (ΔFA) as dependent variables. Our covariates included sex, normalized head motion(framewise displacement) at respective time point(s), age at TP1, age difference between TP1 and TP2, and CPRS symptom score at TP1(Table S1, Figure S4). Our main analyses first examined combined symptom scores and, if significant, subsequent analyses examined whether effects were driven by HI or IA.

We used PALM to account for the lack of independence in the data due to sibling relationships and shared variance between families, constraining permutation tests between families of the same sizes(Winkler, Ridgway, Webster, Smith, & Nichols, 2014). We designed multi-level exchangeability blocks which did not allow permutation among all individuals; permutations were constrained both at the whole-block level (i.e. permute between families of the same size) and the within-block level (i.e. permute within families)(Figure S5). We corrected for multiple testing by running 5000 permutations and threshold-free cluster enhancement(TFCE) as implemented in PALM, part of the FSL toolbox (https://fsl.fmrib.ox.ac.uk/fsl/fslwiki/PALM)(Smith & Nichols, 2009). Results with TFCE-corrected $P<0.05$ were considered statistically significant. All tests used the standard parameter settings for height, extent, and connectivity: H=2, E=1, C=26. We used the Johns Hopkins University DTI-based WM atlas (https://fsl.fmrib.ox.ac.uk/fsl/fslwiki/Atlases) to relate significant clusters to known WM tracts.

Results

Symptom change over time

In Table 1, we present mean symptom scores for HI, IA, and combined (HI+IA). Combined symptom scores significantly decreased over time ($t(98)=4.884, P_{FWE}=2.027\times10^{-6}$). This was due to decreases in both IA scores ($t(98)=4.226, P_{FWE}=2.672\times10^{-5}$) and HI scores ($t(98)=4.394, P_{FWE}=1.410\times10^{-5}$), with a mean decrease of 2.04(SD=4.80) in IA, and 1.46(SD=3.30) in HI score.

Symptom change in relation to WM microstructure at two time-points

As a point of reference: Participants who showed relatively more symptom remission had FA values that moved neither towards nor away from that of those who were diagnosed as never affected; their global FA values increased over time at a similar rate as the never affected individuals, while those who essentially persisted or developed more symptoms over time showed a slightly steeper increase in FA than the other two groups (Figure S6).

Our models demonstrated no significant association between combined symptom score remission and FA_{TP1}, but there was a significant negative association between combined symptom score remission and FA_{TP2} in two regions according to the atlas: lSLF(P_{FWE}=0.038) and lCST(P_{FWE}=0.044)(Table 2;Figure 3A). This was mainly driven by a negative effect of HI dimension score on FA in lCST(P_{FWE}=0.049)(Table 2;Figure 3B).

Additionally, there was a negative trend association between combined symptom score difference and FA difference (P_{FWE}=0.079). Because our one model with a significant effect, as well as those previously reported in an overlapping sample at an earlier time window, were driven by HI, we performed an exploratory *post-hoc* analysis on symptom score difference and FA difference with only HI dimension scores(Brouwer et al., 2020; Damatac et al., 2020; Francx, Zwiers, et al., 2015). Our exploratory results show that larger HI symptom decrease

237 was associated with a larger decrease in FA over time in ten clusters spread over six WM
238 tracts(Table S2, Figure S7).

239 *Post hoc tests of confounders and demographics*

240 Sex, normalized head motion at respective time point(s), age at TP1, age difference between
241 TP1 and TP2, and CPRS symptom score at TP1 were included as covariates in all models. We
242 report main effects after the removal of non-significant interaction effects in Table 2. We found
243 neither a significant main effect nor an interaction effect of any of these covariates with ΔCPRS
244 for all analyses reported above(Table S3).

245 Discussion

246 In this longitudinal investigation of ADHD and WM microstructure, we report that higher
247 symptom decrease is associated with lower FA at follow-up in lCST and lSLF, an effect mainly
248 driven by HI symptom decrease. Thereby, we have essentially replicated and extended the
249 findings reported by Francx, Zwiers, et al. (2015) at an older age range, contributing to the
250 growing body of evidence describing the progression of ADHD and its relation with WM.
251 Additionally, we utilized an improved statistical method to account for the family structure in
252 our data, thus confirming that previous results in this cohort were not confounded by within-
253 family correlations(Winkler et al., 2015). By substantiating those earlier findings, with
254 replication in participants at an older age, and upon better accounting for family relatedness,
255 we conclude that a decrease in symptoms from early adolescence is associated with lower FA
256 in late adolescence and young adulthood.

257 Our longitudinal design of two diagnostic and two DWI time-points allows us to
258 speculate about the chronology of brain changes versus symptom changes. First, we found no
259 evidence that baseline FA predicts ADHD symptom change over time. Second, though a
260 natural expectation would be that more remission leads to higher FA, we found the opposite,

261 somewhat paradoxical result: Greater ADHD symptom decrease was associated with lower FA
262 at follow-up in lSLF and lCST. Third, we found that HI, not IA, symptom decrease was the
263 main driver behind the association with reduced FA in lCST. WM microstructure can change
264 in response to behavior or learning (i.e. plasticity). It is possible that decreased (motor)
265 hyperactivity is associated with less use of corticospinal and motor tracts, which may lead to
266 decreased FA in this area at TP2. Overall, lower FA in both tracts appears to follow, rather than
267 precede, symptom decrease. Speculatively, this suggests that the WM changes may be a
268 downstream result, rather than a cause, of symptom remission in ADHD.

269 FA is an indirect reflection of microstructure and some neuronal processes that improve
270 anatomical connectivity may paradoxically manifest as decreased FA in some locations—
271 especially in principal WM highways through which several fibers cross, like the SLF and
272 CST. At the axonal level, more sprouting, pruning, crossing fibers or fiber dispersion in those
273 tracts during maturation may demonstrate as reduced FA over time. Plasticity in myelin or axon
274 integrity in less dominant fibers could also exhibit as reduced FA in voxels containing multiple
275 fiber orientations. In our participants whose symptoms persisted, higher FA could be the
276 outcome of brain reorganization in less dominant fiber tracts, particularly in those that traverse
277 the CST and SLF. Event-related and resting-state functional MRI studies that grouped their
278 subjects categorically have reported that remitters have stronger connectivity than
279 persisters(Clerkin et al., 2013; Francx, Oldehinkel, et al., 2015). Lower functional connectivity
280 in certain tracts may be related to higher FA in other tracts and vice versa. In a top-down
281 fashion, remitters may learn compensatory strategies to overcome their ADHD symptoms as
282 they age, while persisters may either learn disadvantageous strategies, other beneficial
283 compensatory strategies, or none at all, leading to divergent trajectories of WM development
284 in various brain regions in individuals with persistent ADHD symptoms(Wetterling et al.,
285 2015).

One can find in the literature several instances wherein the SLF and CST are implicated in ADHD. The SLF generally subserves a wide variety of functions related to language, attention, memory, emotion, and visuospatial function; many studies have pointed to its function in visuospatial awareness, as well as attentional selection of sensory content(Conner et al., 2018; Shaw et al., 2015; Wolfers et al., 2015). Our findings are partly in accordance with those of others that have found neurodevelopmental effects linked with unilaterally compromised lSLF maturation during adolescence(Peters et al., 2012). Thus, ADHD symptom persistence may influence higher unilateral SLF integrity as a person develops from early adolescence to young adulthood. The CST integrates cortical and lower brain processing centers in the motor system, has an important role in modulating sensory information, and may be particularly relevant to motor hyperactivity in ADHD(Moreno-López, Olivares-Moreno, Cordero-Erausquin, & Rojas-Piloni, 2016). Altered modulation of sensory information could potentially be involved in HI remission, as the CST contains fibers running from the primary motor, premotor, supplementary motor, somatosensory, parietal and cingulate cortex to the spine and is thus involved in the control of complex voluntary distal movements(Welniarz, Dusart, & Roze, 2017). Correspondingly, the persistence of HI could, indeed, result in increased FA in CST through time. Our unilateral findings may have risen from the fact that 88% of our subjects were right-handed, and most CST axons cross to the contralateral side at the pyramidal decussation before reaching lower motor neurons(Welniarz et al., 2017). We found no evidence that handedness was correlated with change in symptom scores (Table S4).

Based on previous investigations that have similarly found effects of ADHD symptoms on WM microstructure driven by HI, we also conducted an exploratory analysis of only HI symptom remission effects on change in FA(Damatac et al., 2020; Francx, Zwiers, et al., 2015). Our results may suggest that HI symptom remission is associated with more decrease in FA over time. Most of the associations we found were clustered in prefrontal and frontostriatal

311 regions. Higher functional connectivity in prefrontal networks in young adults has been
312 associated with more improvement in symptoms over time(Clerkin et al., 2013; Francx, Zwiers,
313 et al., 2015). Likewise, the prefrontal cortex and its connections are especially important in the
314 remission or persistence of ADHD symptoms(Francx, Oldehinkel, et al., 2015; Halperin &
315 Schulz, 2006). As it continues to develop throughout adolescence, the prefrontal cortex can
316 potentially compensate for the initial causes of ADHD through its connectivity with subcortical
317 regions such as the striatum. Indeed, a study using independent component analysis
318 demonstrated that ADHD diagnosis was significantly associated with reduced brain volume in
319 a component that mapped to the frontal lobes, the striatum, and their interconnecting WM
320 tracts(Cupertino et al., 2019). Although exploratory and tentative, our finding of decreased FA
321 in frontostriatal regions coinciding with HI symptom remission is thus in line with Halperin &
322 Schulz's theory (2006): Neural plasticity and the development of the prefrontal cortex and
323 interconnected neural circuits facilitate recovery over the course of development.

324 We used a dimensional approach in defining the ADHD phenotype, in line with our
325 recent findings in a large overlapping cohort wherein no evidence was found for altered FA in
326 association with categorical ADHD diagnosis(Damatac et al., 2020). Unaffected participants
327 clustered at the low end of the score distribution. Given the relatively small number of fully
328 remitted patients (N=5), together with a subset of 'partly remitted' individuals, our use of
329 symptom severity as a continuous variable maximized power to detect symptom-related
330 changes, while also circumventing arbitrary decisions on the definition of remission(Du Rietz
331 et al., 2016). We thus interpret our findings in terms of symptom severity, reflecting the degree
332 of remission in ADHD patients as well as variation in individuals who do not reach diagnostic
333 threshold.

334 Head motion is quite typical in the ADHD population and is hence a common confound
335 in such studies(Aoki et al., 2018; Yendiki, Koldewyn, Kakunoori, Kanwisher, & Fischl, 2014;

Zwiers, 2010). A previous meta-analysis of DWI studies in ADHD found that most investigations that controlled for head motion did not have significant results(Aoki et al., 2018). We normalized head motion and included it as a confound covariate in all of our analyses, as well as checked each model for an interaction effect with the head motion parameter. We found no evidence that it had an influence on our results.

FA estimates can be less accurate in brain regions consisting of so-called “kissing” and/or crossing fibers, like the CST and SLF. FA gives only one value for the overall restriction of anisotropy in a voxel, which could be a crucial aspect in the inconsistency of findings in the literature regarding WM and ADHD. Future studies may include complementary longitudinal region-of-interest tractography analyses in the clusters that we found to be significant, or by using DWI methods that deliver greater resolution at the neurite level. Techniques that utilize orientation dispersion indices or WM fiber density could potentially provide clarity in the constant discourse of how crossing fibers can mar inferences about FA and brain effects of ADHD. Likewise, incorporating additional DWI data from more than two time points throughout development would, naturally, increase statistical power and enhance our understanding of the dynamic interplay between disorder and development. Due to the wide age range in our sample, we checked for but did not find interactions with baseline age. Nonetheless, more complex, nonlinear patterns with age may exist across the age ranges we studied. We cannot assume that the relationship between symptom change and brain change is a constant process throughout the entire age range in this study.

Conclusion

We used two DWI time-points in a longitudinal study of dimensional symptom scores in ADHD. Our results indicate that, in specific WM tracts, greater symptom improvement results in lower FA at follow-up. We show that WM alterations may occur downstream of symptom change. The effects we have found confirm and extend earlier findings in an overlapping

361 sample; they indicate divergent trajectories of WM development in individuals with persistent
362 ADHD symptoms compared to those showing remittance, and support the role of prefrontal
363 and sensorimotor development in the symptom remission of ADHD.

364 Acknowledgments

365 The NeuroIMAGE study was supported by National Institutes of Health Grant No.
366 R01MH62873 (to Stephen V. Faraone), NWO Large Investment Grant No. 1750102007010
367 (to JKB), NWO Brain & Cognition Grant Nos. 056-13-015 (to JKB) and 433-09-242 (to JKB),
368 ZonMW Grant No. 60-60600-97-193 (to JKB), and a matching grant from Radboud University
369 Medical Center.

370 Correspondence

371
372 Christienne G. Damatac, Department of Cognitive Neuroscience, Donders Centre for
373 Cognition, Donders Institute for Brain, Cognition and Behaviour, Kapittelweg 29, 6525 EN
374 Nijmegen, The Netherlands; Email: c.gonzalesdamatac@donders.ru.nl

375

Key points

- Attention-deficit hyperactivity disorder is associated with white matter microstructure, but little is known about how they are longitudinally related as a child develops into adulthood.
- We used voxel-wise Tract-Based Spatial Statistics with permutation-based inference to investigate how symptom score change relates to fractional anisotropy in individuals with ADHD and typically developing controls over a period of about four years.
- We provided for the first time, evidence that altered FA appears to follow, rather than precede, changes in symptom remission.
- Our findings indicate divergent white matter developmental trajectories between individuals with persistent and remittent ADHD, and support the role of prefrontal and sensorimotor tracts in the remission of ADHD.

References

American Psychiatric Association. (2013). *American Psychiatric Association, 2013. Diagnostic and statistical manual of mental disorders (5th ed.). American Journal of Psychiatry*.

Aoki, Y., Cortese, S., & Castellanos, F. X. (2018). Research Review: Diffusion tensor imaging studies of attention-deficit/hyperactivity disorder: meta-analyses and reflections on head motion. *Journal of Child Psychology and Psychiatry and Allied Disciplines*, *59*(3), 193–202.

Beaulieu, C. (2002). The basis of anisotropic water diffusion in the nervous system - A technical review. *NMR in Biomedicine*, *15*(7–8), 435–455.

Brouwer, R. M., Klein, M., Grasby, K. L., Schnack, H. G., Jahanshad, N., Teeuw, J., Thomopoulos, S. I., et al. (2020). Dynamics of Brain Structure and its Genetic Architecture over the Lifespan. *bioRxiv*.

Clerkin, S. M., Schulz, K. P., Berwid, O. G., Fan, J., Newcorn, J. H., Tang, C. Y., & Halperin, J. M. (2013). Thalamo-cortical activation and connectivity during response preparation in adults with persistent and remitted ADHD. *American Journal of Psychiatry*, *170*(9), 1011–1019.

Conner, A. K., Briggs, R. G., Rahimi, M., Sali, G., Baker, C. M., Burks, J. D., Glenn, C. A., et al. (2018). A Connectomic Atlas of the Human Cerebrum—Chapter 10: Tractographic Description of the Superior Longitudinal Fasciculus. *Operative Neurosurgery*, *15*(suppl_1), S407–S422.

Conners, C. K., Erhardt, D., Epstein, J. N., Parker, J. D. A., Sitarenios, G., & Sparrow, E. (1999). Self-ratings of ADHD symptoms in adults I: Factor structure and normative data. *Journal of Attention Disorders*.

Cortese, S., Imperati, D., Zhou, J., Proal, E., Klein, R. G., Mannuzza, S., Ramos-Olazagasti, M. A., et al. (2013). White matter alterations at 33-year follow-up in adults with childhood attention-deficit/hyperactivity disorder. *Biological psychiatry*, *74*(8), 591–8. Retrieved from http://www.ncbi.nlm.nih.gov/pubmed/23566821

Cupertino, R. B., Soheili-Nezhad, S., Grevet, E. H., Bandeira, C. E., Picon, F. A., Tavares, M. E., Naaijen, J., et al. (2019). Reduced fronto-striatal volume in ADHD in two cohorts across the lifespan. *bioRxiv*.

Damatac, C. G., Chauvin, R. J. M., Zwiers, M. P., van Rooij, D., Akkermans, S. E. A., Naaijen, J., Hoekstra, P. J., et al. (2020). White Matter Microstructure in Attention-Deficit/Hyperactivity Disorder: A Systematic Tractography Study in 654 Individuals. *Biological Psychiatry: Cognitive Neuroscience and Neuroimaging*, 1–10. Elsevier Inc. Retrieved from https://doi.org/10.1016/j.bpsc.2020.07.015

van Duijvenvoorde, A. C. K., Westhoff, B., de Vos, F., Wierenga, L. M., & Crone, E. A. (2019). A three-wave longitudinal study of subcortical–cortical resting-state

connectivity in adolescence: Testing age- and puberty-related changes. *Human Brain Mapping*, *40*(13), 3769–3783.

van Ewijk, H., Heslenfeld, D. J., Zwiers, M. P., Faraone, S. V., Luman, M., Hartman, C. A., Hoekstra, P. J., et al. (2014). Different mechanisms of white matter abnormalities in attention-deficit/ hyperactivity disorder: A diffusion tensor imaging study. *Journal of the American Academy of Child and Adolescent Psychiatry*, *53*(7), 790-799.e3. Elsevier Inc. Retrieved from http://dx.doi.org/10.1016/j.jaac.2014.05.001

Faraone, S. V, Asherson, P., Banaschewski, T., Biederman, J., Buitelaar, J. K., Ramos-Quiroga, J. A., Rohde, L. A., et al. (2015). Attention-deficit/hyperactivity disorder. *Nature reviews. Disease primers*, *1*, 15020. Radboud University Medical Center, Donders Institute for Brain, Cognition and Behaviour, Departments of Human Genetics and Psychiatry, Nijmegen, The Netherlands. Retrieved from http://eutils.ncbi.nlm.nih.gov/entrez/eutils/elink.fcgi?dbfrom=pubmed&id=27189265&retmode=ref&cmd=prlinks

Francx, W., Oldehinkel, M., Oosterlaan, J., Heslenfeld, D., Hartman, C. A., Hoekstra, P. J., Franke, B., et al. (2015). The executive control network and symptomatic improvement in attention-deficit / hyperactivity disorder. *Cortex*, *73*, 62–72. Elsevier Srl. Retrieved from http://dx.doi.org/10.1016/j.cortex.2015.08.012

Francx, W., Zwiers, M. P., Mennes, M., Oosterlaan, J., Heslenfeld, D., Hoekstra, P. J., Hartman, C. A., et al. (2015). White matter microstructure and developmental improvement of hyperactive/impulsive symptoms in attention-deficit/hyperactivity disorder. *Journal of Child Psychology and Psychiatry and Allied Disciplines*, *56*(12), 1289–1297. Karakter Child and Adolescent Psychiatry University Centre, Nijmegen, The Netherlands. Retrieved from http://doi.wiley.com/10.1111/jcpp.12379

Franke, B., Michelini, G., Asherson, P., Banaschewski, T., Bilbow, A., Buitelaar, J. K.,

Cormand, B., et al. (2018). Live fast , die young ? A review on the developmental trajectories of ADHD across the lifespan. *European Neuropsychopharmacology*, *28*(10), 1059–1088. Elsevier B.V. Retrieved from https://doi.org/10.1016/j.euroneuro.2018.08.001

Giorgio, A., Watkins, K. E., Douaud, G., James, A. C., James, S., De Stefano, N., Matthews, P. M., et al. (2008). Changes in white matter microstructure during adolescence. *NeuroImage*, *39*(1), 52–61.

Halperin, J. M., & Schulz, K. P. (2006). Revisiting the role of the prefrontal cortex in the pathophysiology of attention-deficit/hyperactivity disorder. *Psychological bulletin*, *132*(4), 560–581. Department of Psychology, Queens College of the City University of New York, Flushing, NY 11367, USA. jeffrey.halperin@qc.cuny.edu. Retrieved from http://eutils.ncbi.nlm.nih.gov/entrez/eutils/elink.fcgi?dbfrom=pubmed&id=16822167&retmode=ref&cmd=prlinks

Hoogman, M., Bralten, J., Hibar, D. P., Mennes, M., Zwiers, M. P., Schweren, L. S. J., van Hulzen, K. J. E., et al. (2017). Subcortical brain volume differences in participants with attention deficit hyperactivity disorder in children and adults: a cross-sectional mega-analysis. *The Lancet Psychiatry*, *4*(4), 310–319.

Kochunov, P., Williamson, D. E., Lancaster, J., Fox, P., Cornell, J., Blangero, J., & Glahn, D. C. (2012). Fractional anisotropy of water diffusion in cerebral white matter across the lifespan. *Neurobiology of Aging*, *33*(1), 9–20. Retrieved from https://linkinghub.elsevier.com/retrieve/pii/S0197458010000448

Lahey, B. B., & Willcutt, E. G. (2010). Predictive Validity of a Continuous Alternative to Nominal Subtypes of Attention-Deficit/Hyperactivity Disorder for DSM – V. *Journal of Clinical Child & Adolescent Psychology*, *39*(6), 761–775. Retrieved from http://www.tandfonline.com/doi/abs/10.1080/15374416.2010.517173

Lebel, C., & Deoni, S. (2018). The development of brain white matter microstructure. *NeuroImage*, *182*(3), 207–218. Retrieved from https://linkinghub.elsevier.com/retrieve/pii/S1053811917311217

Madhyastha, T., Mérillat, S., Hirsiger, S., Bezzola, L., Liem, F., Grabowski, T., & Jäncke, L. (2014). Longitudinal reliability of tract-based spatial statistics in diffusion tensor imaging. *Human Brain Mapping*, *35*(9), 4544–4555.

Marcus, D. K., & Barry, T. D. (2011). Does attention-deficit/hyperactivity disorder have a dimensional latent structure? A taxometric analysis. *Journal of Abnormal Psychology*, *120*(2), 427–442. Retrieved from http://doi.apa.org/getdoi.cfm?doi=10.1037/a0021405

Moreno-López, Y., Olivares-Moreno, R., Cordero-Erausquin, M., & Rojas-Piloni, G. (2016). Sensorimotor integration by corticospinal system. *Frontiers in Neuroanatomy*, *10*(MAR), 1–6.

Müller, U. C., Asherson, P., Banaschewski, T., Buitelaar, J. K., Ebstein, R. P., Eisenberg, J., Gill, M., et al. (2011a). The impact of study design and diagnostic approach in a large multi-centre ADHD study. Part 1: ADHD symptom patterns. *BMC Psychiatry*, *11*(1), 54. BioMed Central Ltd. Retrieved from http://bmcpsychiatry.biomedcentral.com/articles/10.1186/1471-244X-11-54

Müller, U. C., Asherson, P., Banaschewski, T., Buitelaar, J. K., Ebstein, R. P., Eisenberg, J., Gill, M., et al. (2011b). The impact of study design and diagnostic approach in a large multi-centre ADHD study: Part 2: Dimensional measures of psychopathology and intelligence. *BMC Psychiatry*, *11*(1), 55. BioMed Central Ltd.

Paus, T., Collins, D. L., Evans, A. C., Leonard, G., Pike, B., & Zijdenbos, A. (2001). Maturation of white matter in the human brain: A review of magnetic resonance studies. *Brain Research Bulletin*, *54*(3), 255–266.

Peters, B. D., Szeszko, P. R., Radua, J., Ikuta, T., Gruner, P., Derosse, P., Zhang, J. P., et al.

(2012). White matter development in adolescence: Diffusion tensor imaging and meta-analytic results. *Schizophrenia Bulletin*, *38*(6), 1308–1317.

von Rhein, D., Mennes, M., van Ewijk, H., Groenman, A. P., Zwiers, M. P., Oosterlaan, J., Heslenfeld, D., et al. (2015). The NeuroIMAGE study: a prospective phenotypic, cognitive, genetic and MRI study in children with attention-deficit/hyperactivity disorder. Design and descriptives. *European Child and Adolescent Psychiatry*, *24*(3), 265–281. Centre for Cognitive Neuroscience, Donders Institute for Brain, Cognition and Behaviour, Radboud University Medical Centre, Nijmegen, The Netherlands, Daniel.vonRhein@gmail.com. Retrieved from http://eutils.ncbi.nlm.nih.gov/entrez/eutils/elink.fcgi?dbfrom=pubmed&id=25012461&retmode=ref&cmd=prlinks

Du Rietz, E., Cheung, C. H. M., McLoughlin, G., Brandeis, D., Banaschewski, T., Asherson, P., & Kuntsi, J. (2016). Self-report of ADHD shows limited agreement with objective markers of persistence and remittance. *Journal of Psychiatric Research*.

Shaw, P., Sudre, G., Wharton, A., Weingart, D., Sharp, W., & Sarlls, J. (2015). White matter microstructure and the variable adult outcome of childhood attention deficit hyperactivity disorder. *Neuropsychopharmacology*, *40*(3), 746–754. Nature Publishing Group. Retrieved from http://dx.doi.org/10.1038/npp.2014.241

Smith, S. M., Jenkinson, M., Johansen-berg, H., Rueckert, D., Nichols, T. E., Mackay, C. E., Watkins, K. E., et al. (2006). Tract-based spatial statistics: Voxelwise analysis of multi-subject diffusion data. *NeuroImage*, *31*(4), 1487–1505.

Smith, S. M., & Nichols, T. E. (2009). Threshold-free cluster enhancement: Addressing problems of smoothing, threshold dependence and localisation in cluster inference. *NeuroImage*, *44*(1), 83–98. Elsevier Inc.

Sudre, G., Mangalmurti, A., & Shaw, P. (2018). Growing out of attention deficit

516 hyperactivity disorder: Insights from the ‘remitted’ brain. *Neuroscience and*
517 *Biobehavioral Reviews*, *94*(September), 198–209.
518 Welniarz, Q., Dusart, I., & Roze, E. (2017). The corticospinal tract: Evolution, development,
519 and human disorders. *Developmental Neurobiology*, *77*(7), 810–829.
520 Wetterling, F., Mccarthy, H., Tozzi, L., Skokauskas, N., O’Doherty, J. P., Mulligan, A.,
521 Meaney, J., et al. (2015). Impaired reward processing in the human prefrontal cortex
522 distinguishes between persistent and remittent attention deficit hyperactivity disorder.
523 *Human Brain Mapping*, *36*(11), 4648–4663.
524 Winkler, A. M., Ridgway, G. R., Webster, M. A., Smith, S. M., & Nichols, T. E. (2014).
525 Permutation inference for the general linear model. *NeuroImage*, *92*, 381–397. The
526 Authors.
527 Winkler, A. M., Webster, M. A., Vidaurre, D., Nichols, T. E., & Smith, S. M. (2015). Multi-
528 level block permutation. *NeuroImage*, *123*, 253–268. The Authors.
529 Wolfers, T., Onnink, A. M. H., Zwiers, M. P., Arias-Vasquez, A., Hoogman, M., Mostert, J.
530 C., Kan, C. C., et al. (2015). Lower white matter microstructure in the superior
531 longitudinal fasciculus is associated with increased response time variability in adults
532 with attentiondeficit/hyperactivity disorder. *Journal of Psychiatry and Neuroscience*,
533 *40*(5), 344–351.
534 Yendiki, A., Koldewyn, K., Kakunoori, S., Kanwisher, N., & Fischl, B. (2014). Spurious
535 group differences due to head motion in a diffusion MRI study. *NeuroImage*, *88*(88),
536 79–90. Retrieved from https://linkinghub.elsevier.com/retrieve/pii/S1053811913011312
537 Zwiers, M. P. (2010). NeuroImage Patching cardiac and head motion artefacts in diffusion-
538 weighted images. *NeuroImage*, *53*(2), 565–575. Elsevier Inc. Retrieved from
539 http://dx.doi.org/10.1016/j.neuroimage.2010.06.014
540

541 **Figures and tables**

542

	TP1		TP2			
	Mean	**(SD)**	**Mean**	**(SD)**	**Test Statistic**	**(*P*)**
Age, years	16.91	(3.47)	20.57	(3.52)		
Sex, female	N = 42	42%	N = 42	42%		
Estimated IQ	105.15	(15.02)	106.44	(16.38)	F(1,100) = 0.84	(0.38)
Head motion, framewise displacement	0.51	(0.35)	0.47	(0.22)	F(1,100) = 2.41	($<10^{-4}$)
Handedness, right	N = 89	89%	N = 89	89%		
CPRS dimension score by diagnostic group						
Combined score	12.76	(12.11)	9.26	(10.20)		
Affected	24.38	(9.63)	18.86	(10.03)		
Subthreshold	8.55	(7.79)	7.13	(7.55)		
Unaffected	4.04	(4.40)	3.06	(4.07)		
Inattention score	8.05	(7.65)	6.02	(6.65)		
Affected	15.05	(5.98)	12.17	(6.55)		
Subthreshold	5.64	(5.35)	4.53	(4.44)		
Unaffected	2.76	(3.82)	2.06	(3.14)		
Hyperactivity-impulsivity score	4.71	(5.30)	3.25	(4.23)		
Affected	9.32	(5.28)	6.69	(4.88)		
Subthreshold	2.91	(3.05)	2.60	(3.20)		
Unaffected	1.28	(1.64)	1.00	(1.65)		
Medication use						
Duration, cumulative days	668	(1,056)	1,161	(1,720)		
Ever used, yes	N = 46	46%	N = 46	46%		

543

Table 1. Demographic and clinical characteristics of the sample at NeuroIMAGE1(TP1) and NeuroIMAGE2(TP2) with mean and standard deviation. Reported values pertain to all participants in the final sample after all quality control(N=99). IQ: estimated at both timepoints using vocabulary and block design subtests of the Wechsler Intelligence Scale for Children(WISC-III) or Wechsler Adult Intelligence Scale(WAIS-III). Combined CPRS symptom score is the sum of two separate dimensions: hyperactivity-impulsivity and inattention. Medications: Ritalin(methylphenidate), Concerta(methylphenidate), Strattera(atomoxetine), and any other ADHD medication. The majority of patients were taking prescription medication for ADHD, mostly methylphenidate or atomoxetine. Medication use duration: lifetime cumulative number of days used on the day of the MRI scan (numerical integer value). Ever used: whether or not participants had ever taken ADHD medication in their lives (binary factor: yes or no).

555

Model	WM tract	N_{voxels}	MNI (Peak voxel)			t_{max}	P_{FWE}
			X_{COG}	Y_{COG}	Z_{COG}		
FA_{TP2} ~ $\Delta CPRS_{combined}$	lCST	723	-21	-27	44	0.755	**0.044**
	lSLF	579	-33	-20	38	0.881	**0.038**
FA_{TP2} ~ $\Delta CPRS_{HI}$	lCST	17	-18	-25	52	0.981	**0.049**

556

557 **Table 2.** TBSS results of significant models: WM tracts, peak voxels, and localization of significant
558 clusters(P_{FWE}<0.05) of voxel-wise permutation based dimensional analyses (see full composition of models in
559 Table S1). N_{voxels}: number of voxels, X/Y/Z_{COG}: location of the center of gravity for the cluster(vox/mm), MNI:
560 Montreal Neurological Institute coordinates, t_{max}: highest threshold-free cluster enhancement t-statistic value per
561 cluster, WM tract: anatomical location in a white matter tract based on the Johns Hopkins University DTI-based
562 white-matter atlases, lCST: left corticospinal tract, lSLF: left superior longitudinal fasciculus. Model FA_{TP2} ~
563 $\Delta CPRS_{combined}$: Less combined symptom score decrease was associated with more FA at follow-up in lSLF and
564 lCST. Model FA_{TP2} ~ $\Delta CPRS_{HI}$: The negative effect in the previous model was driven by HI score remission.

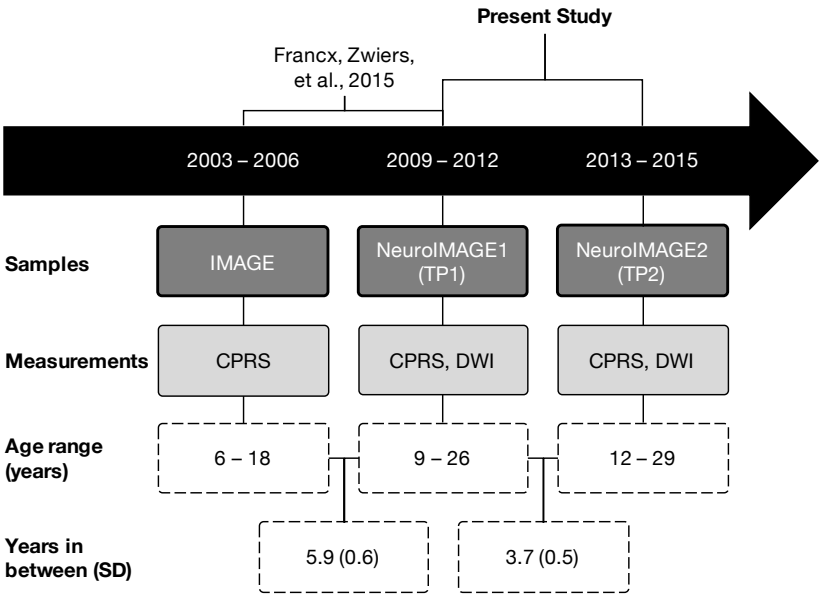

Figure 1. Schematic diagram of how this study chronologically relates to a previous study, samples included, relevant clinical and imaging measurements, study sample age ranges, and mean years (standard deviation) in between each measurement time-point(Francx, Zwiers, et al., 2015; Müller et al., 2011b; von Rhein et al., 2015). The present study is an analysis of TP1 and TP2. DWI: diffusion-weighted imaging, CPRS: Conners Parent Rating Scale(Conners et al., 1999).

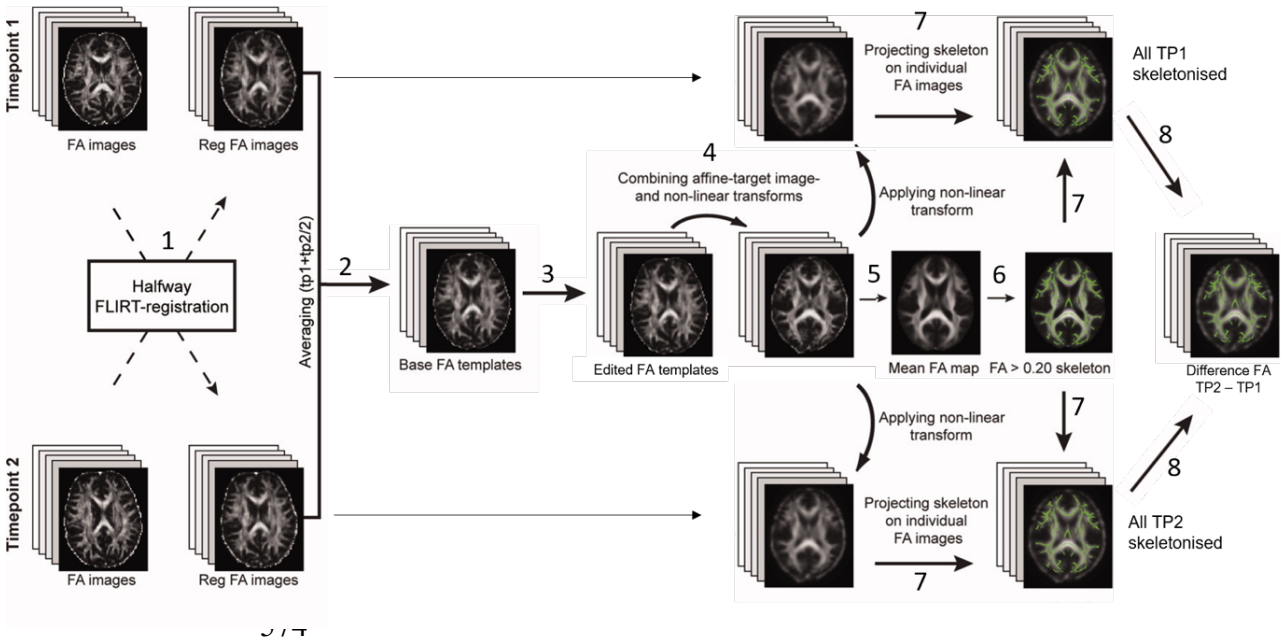

Figure 2. Our longitudinal TBSS pipeline was adapted to create a nonbiased individual subject template for use as a base template (2), which was then non-linearly registered to FMRIB58 FA standard-space (4), to create a mean FA skeleton (5), onto which each subject's aligned FA data from both time points was projected (7).

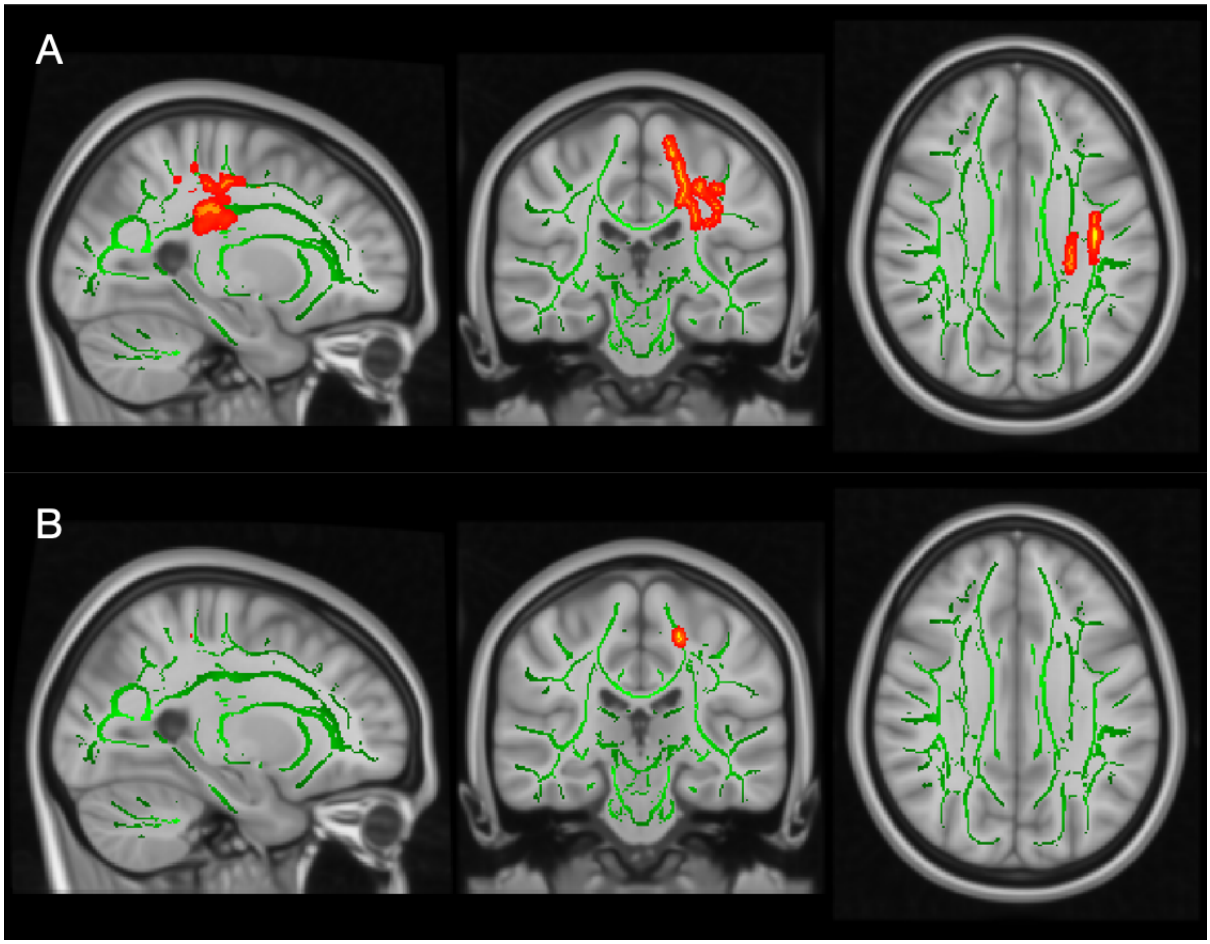

Figure 3. TBSS results showing significant associations (red-yellow) between FA values and the CPRS dimension scores over time. The mean FA skeleton across all subjects (green) was overlain on the MNI template image for presentation (x=-25, y=-25, z=31). Results were thickened for visualization (FSL "tbss_fill") and presented here in radiological convention from sagittal, coronal, and axial perspectives, respectively. **(A)** Lower FA values at follow-up (TP2) were associated with a larger decrease in combined symptom score in the left superior longitudinal fasciculus (lSLF)(P_{FWE}=0.038) and the left corticospinal tract (lCST)(P_{FWE}=0.044); **(B)** Lower FA values at TP2 were associated with a larger decrease in HI symptom score in lCST(P_{FWE}=0.049).

Supplementary materials

Model 1	FA_{TP1}	~	ΔCPRS	+	age_{TP1}	+	Δage	+	sex	+	$CPRS_{TP1}$	+	head $motion_{TP1}$		
Model 2	FA_{TP2}	~	ΔCPRS	+	age_{TP1}	+	Δage	+	sex	+	$CPRS_{TP1}$	+	head $motion_{TP2}$		
Model 3	ΔFA	~	ΔCPRS	+	age_{TP1}	+	Δage	+	sex	+	$CPRS_{TP1}$	+	head $motion_{TP1}$	+	head $motion_{TP2}$

Table S1. Composition of our three general linear models. We essentially have a cross-lagged design with fractional anisotropy (FA) as the dependent variable. The difference in CPRS ($\Delta CPRS = CPRS_{TP1} - CPRS_{TP2}$) is the predictor variable in all models. For each model, CPRS score could be the inattention, hyperactivity-impulsivity, or combined score. The outcome variables of these models are, respectively: FA at baseline (TP1), FA at follow-up (TP2), and change in FA. Permutation analysis (PALM) necessitated that we kept the (TBSS output) FA image as the dependent variable. We covaried for participant baseline age, change in years of age, sex, baseline CPRS symptom score, and framewise displacement head motion at the relevant FA time-point in the dependent variable.

601

Exploratory model	WM tract	N_{voxels}	MNI (Peak voxel) X_{COG}	Y_{COG}	Z_{COG}	t_{max}	P_{FWE}
$\Delta FA \sim \Delta CPRS_{HI}$	lIFOF	508	-29	24	17	0.441	0.041
	lIFOF	376	-17	31	-10	0.613	0.035
	Fmin	339	-18	50	0	0.585	0.042
	lUNC	174	-25	17	-8	0.564	0.045
	lCST	158	-22	-13	8	0.562	0.047
	Fmin	22	-20	38	21	0.563	0.049
	CCG	17	-17	32	23	0.562	0.049
	lIFOF	11	-28	15	-1	0.563	0.049
	Fmin	11	-18	46	17	0.566	0.049
	Fmin	9	-12	41	-17	0.563	0.049

602

603 **Table S2.** Exploratory *post-hoc* analysis results. Greater HI symptom decrease was associated with a larger
604 decrease in FA over time in several WM clusters. P-values reported here were not adjusted for multiple testing.
605 lIFOF: left inferior fronto-occipital fasciculus, Fmin: forceps minor of the corpus callosum, lUNC: left uncinate
606 fasciculus, CCG: cingulum cingulate gyrus.

607

608

Model	WM tract	N_{voxels}	MNI (Peak voxel) X_{COG}	Y_{COG}	Z_{COG}	t_{max}	P_{FWE}	age_{TP1} interaction P
FA_{TP2} ~ $\Delta CPRS_{combined}$	lCST	723	-21	-27	44	0.755	0.044	0.463
	lSLF	579	-33	-20	38	0.881	0.038	0.808
FA_{TP2} ~ $\Delta CPRS_{HI}$	lCST	17	-18	-25	52	0.981	0.049	0.154
ΔFA ~ $\Delta CPRS_{HI}$	lIFOF	508	-29	24	17	0.441	0.041	0.667
	lIFOF	376	-17	31	-10	0.613	0.035	0.055
	Fmin	339	-18	50	0	0.585	0.042	0.874
	lUNC	174	-25	17	-8	0.564	0.045	0.131
	lCST	158	-22	-13	8	0.562	0.047	0.130
	Fmin	22	-20	38	21	0.563	0.049	0.239
	CCG	17	-17	32	23	0.562	0.049	0.238
	lIFOF	11	-28	15	-1	0.563	0.049	0.238
	Fmin	11	-18	46	17	0.566	0.049	0.239
	Fmin	9	-12	41	-17	0.563	0.049	0.237

609

610 **Table S3.** Interaction effects of ΔCPRS and age at TP1 for significant models.

611

612

ΔCPRS score	**Spearman's ρ**	***P***
Combined	0.038	0.709
Hyperactivity-impulsivity	0.098	0.331
Inattention	-0.007	0.948

613

614 **Table S4.** No significant correlation (Spearman's rho) between difference in CPRS score ($\Delta CPRS = CPRS_{TP1} -$

615 $CPRS_{TP2}$) and right-handedness in our sample.

616

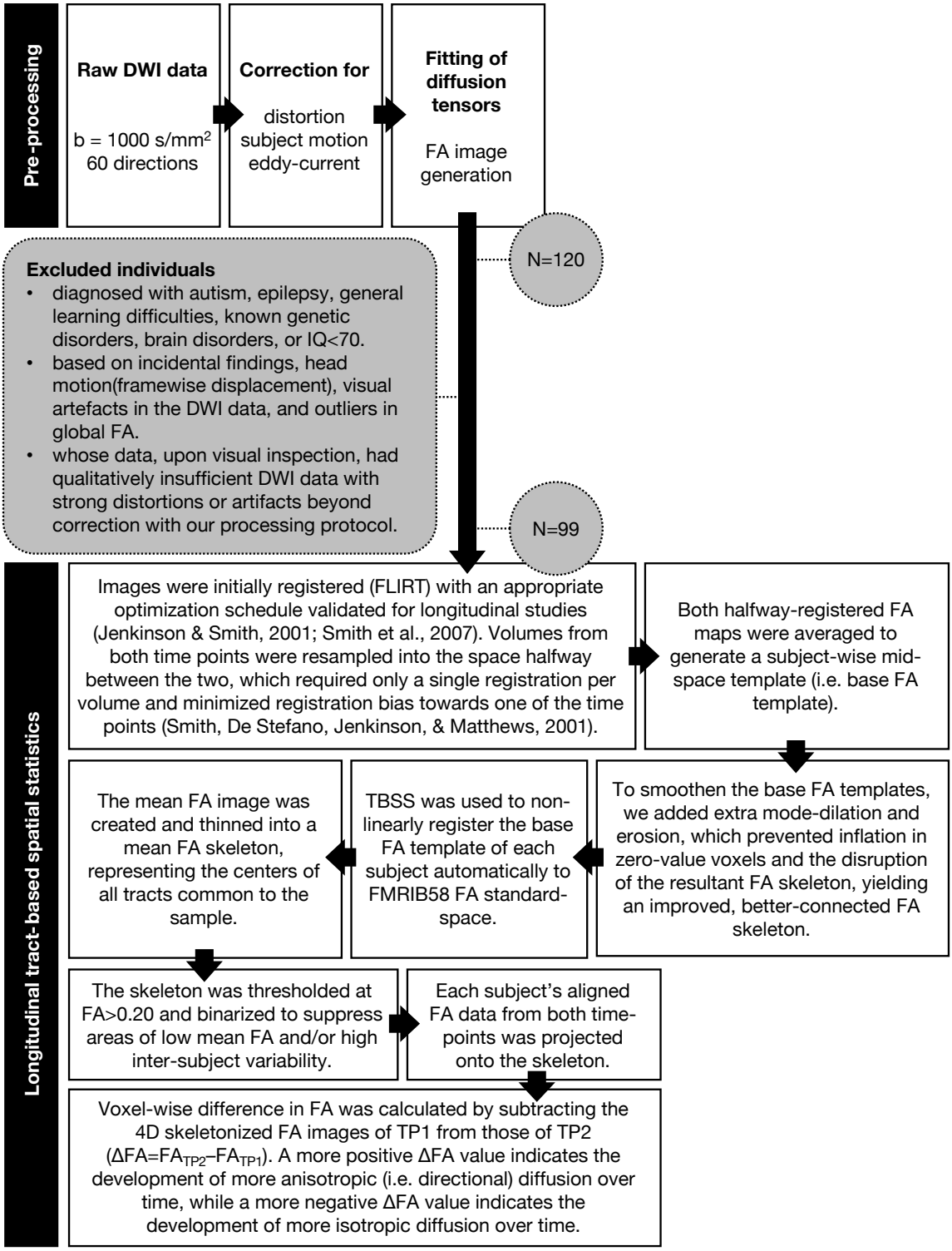

Figure S1. Processing pipeline. During pre-processing, DWI images were realigned and corrected for residual eddy current and for motion artefacts using robust tensor modelling (PATCH)(Zwiers, 2010). Diffusion tensor characteristics and FA values were calculated for each voxel(Behrens et al., 2003). After pre-processing, we used a custom longitudinal TBSS pipeline adapted from others to create non-biased individual subject templates (Madhyastha et al., 2014).

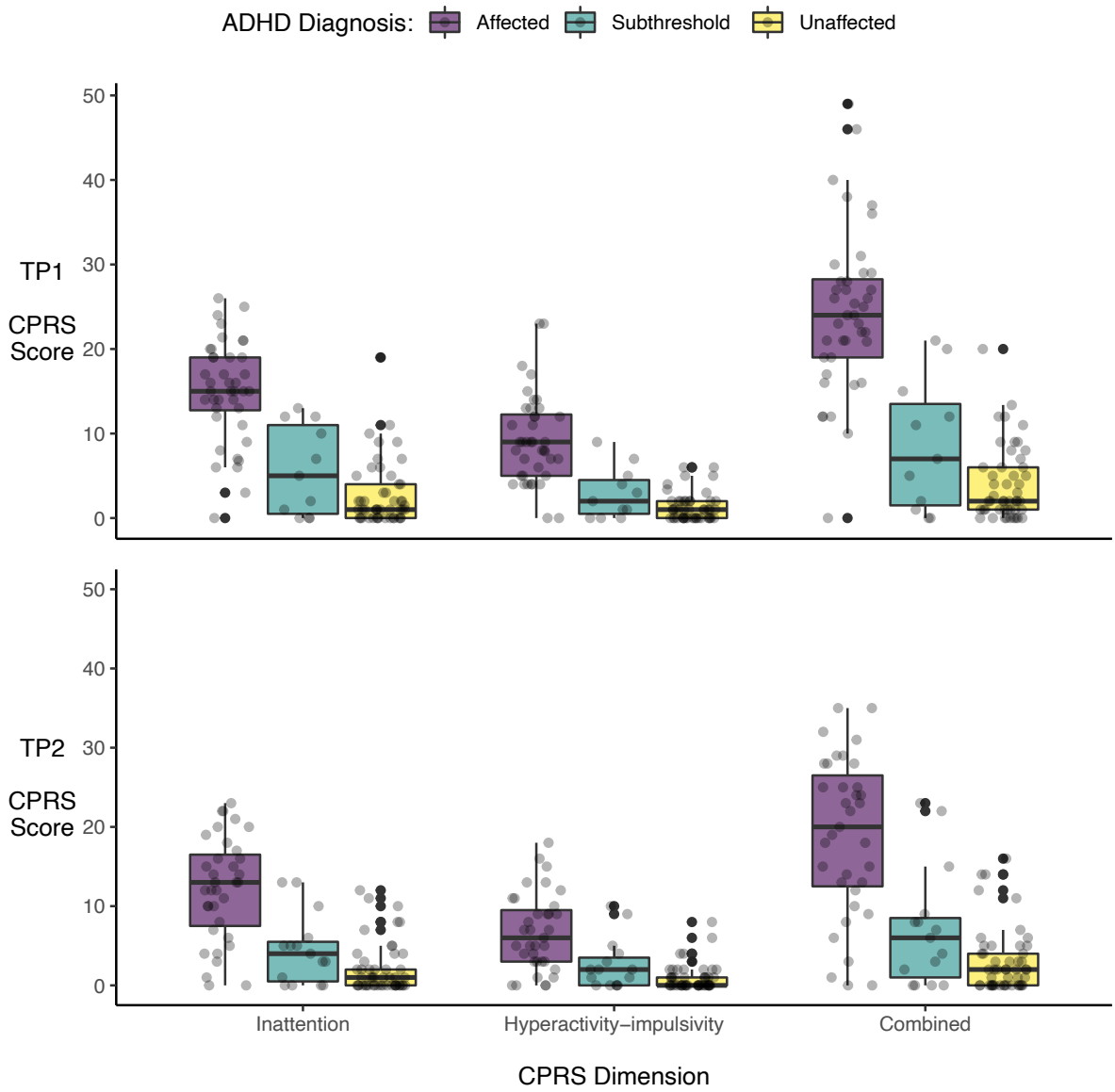

Figure S2. Jittered scatterplots overlain with boxplots of individual Conners Parent Rating Scale (CPRS) dimension scores colored by clinical diagnosis group at baseline (TP1; top panel) and follow-up (TP2; bottom panel).

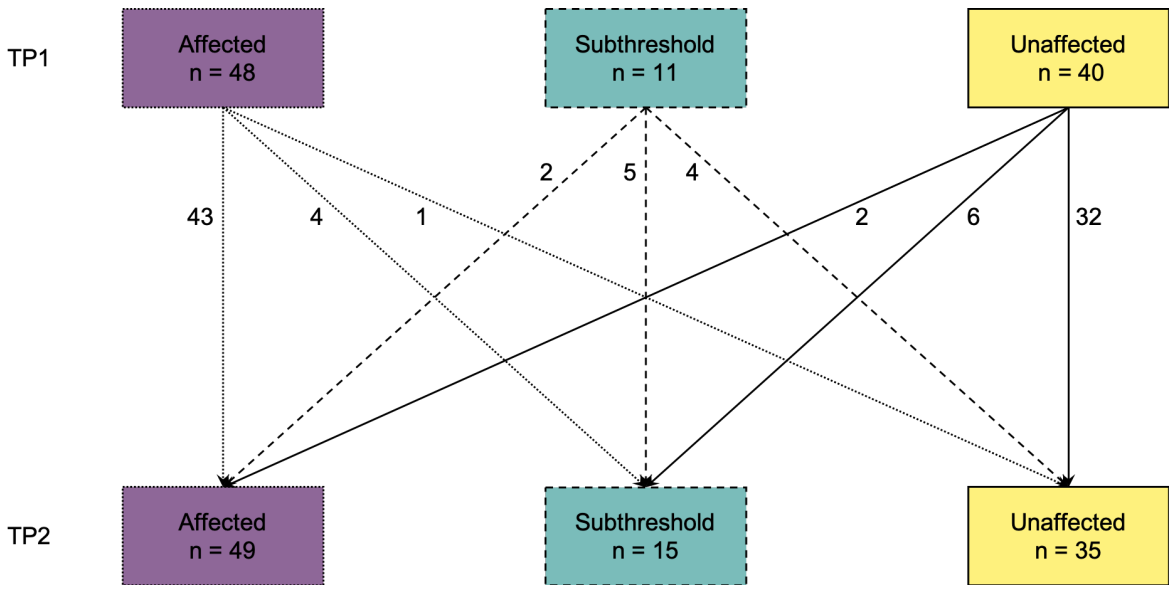

Figure S3. Changes in the diagnostic make-up of our study sample (N=99). Although the total number of participants remained constant, the number of individuals in each diagnosis group changed between time-point 1 (TP1) and time-point 2 (TP2).

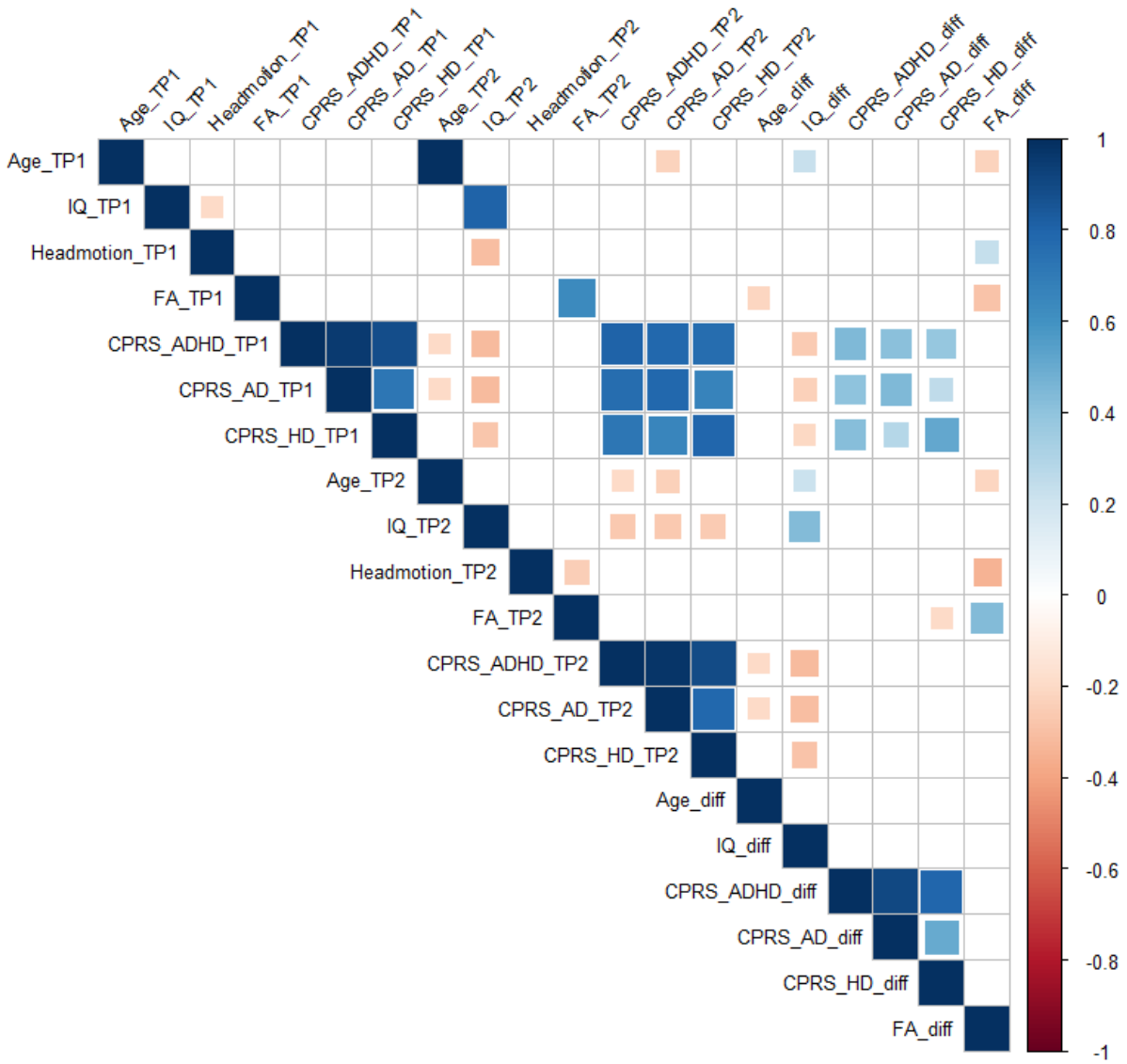

Figure S4. Spearman correlation matrix of independent and dependent variables, as well as covariates. These correlation tests were performed before the main analyses. The color intensity of each box indicates the magnitude of the correlation. Positive correlations are presented in blue and negative correlations in red. The size of the box indicates its significance, with significant correlations filling each square completely.

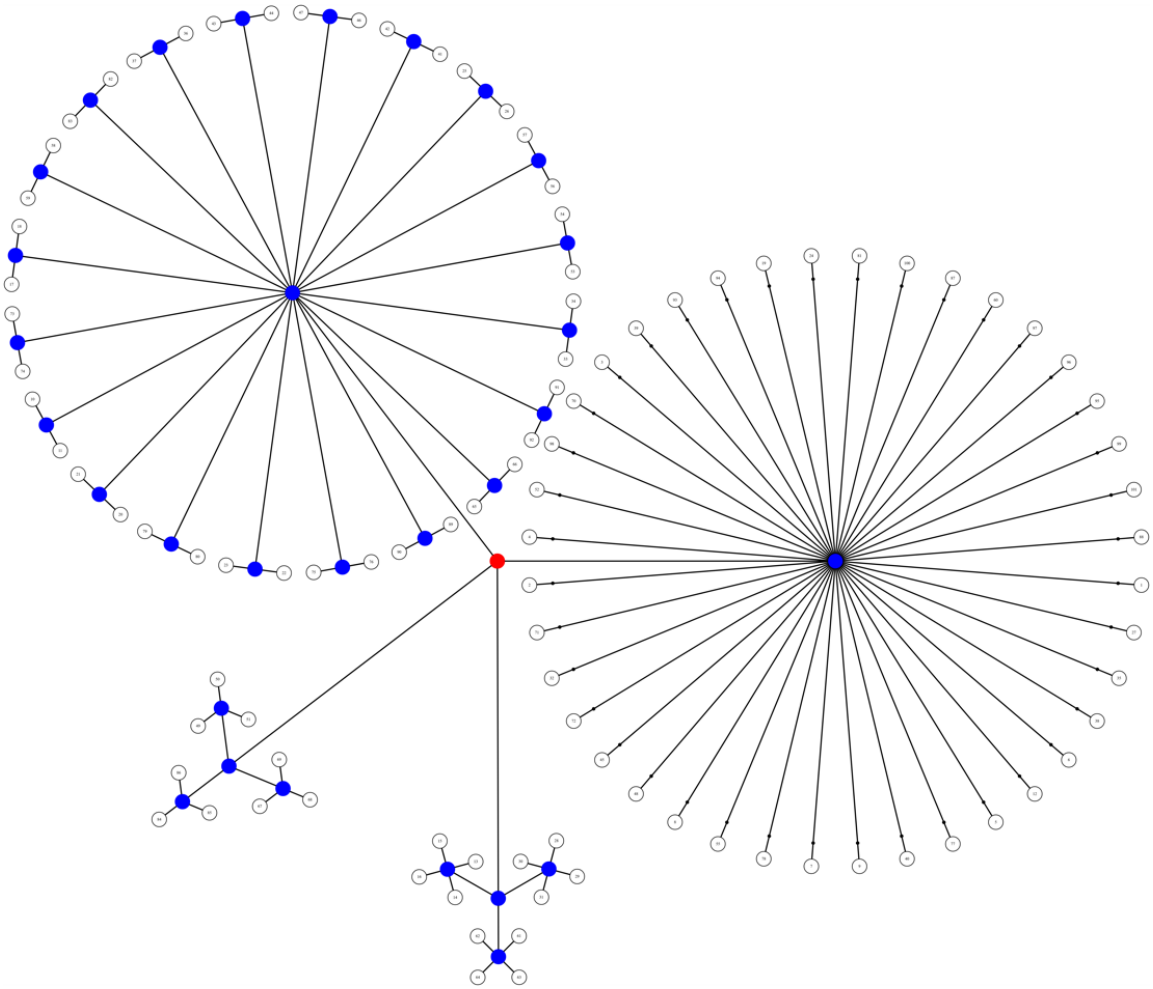

Figure S5. Visual representation of the multi-level notation of family structure in our sample. The four groups represent the size of each family: 3 families of 3 children, 3 families of 4 children, 20 families of 2 children, and 40 families of 1 child in the study. We depict the levels as branches from the central red node, akin to a tree in which the most peripheral elements (leaves) represent the observations. The nodes from which the branches depart either allow (blue) or do not allow (red) permutations.

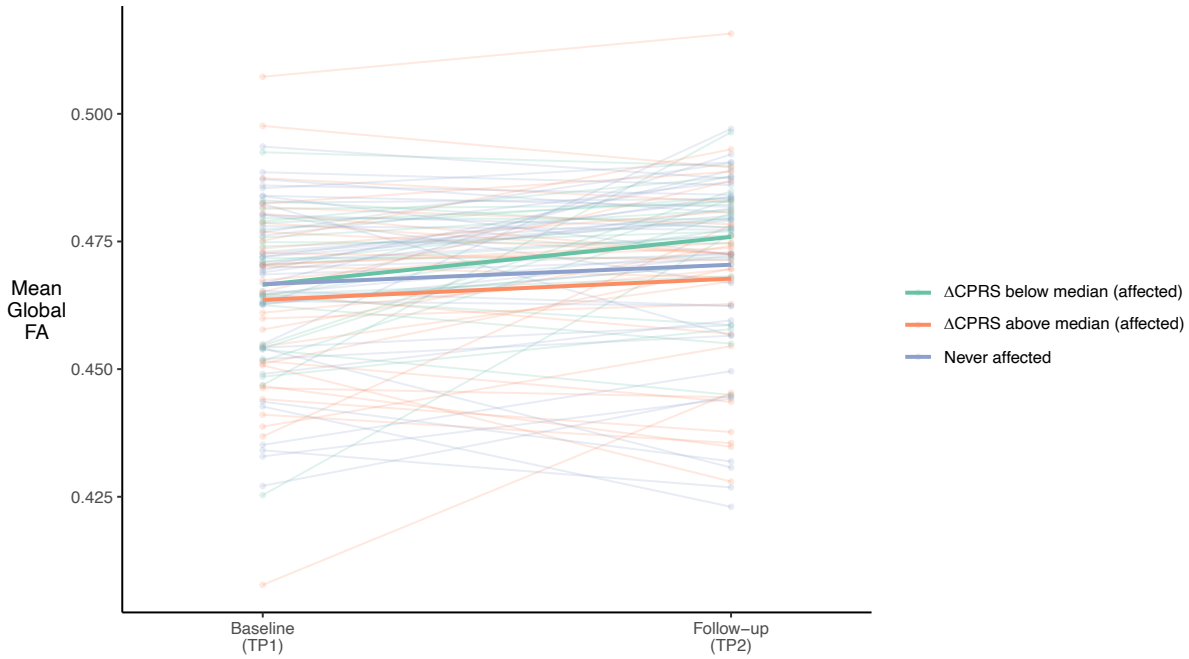

Figure S6. Line plot illustrating individual changes in average whole-brain fractional anisotropy (FA) from baseline to follow-up, grouped by never affected participants (blue) versus affected participants (including subthreshold). Here, affected individuals are further split along the median into two groups according to whether their change in combined Conners Parent Rating Scale score (ΔCPRS) was above (orange) or below (green) the affected sample's median of that change.

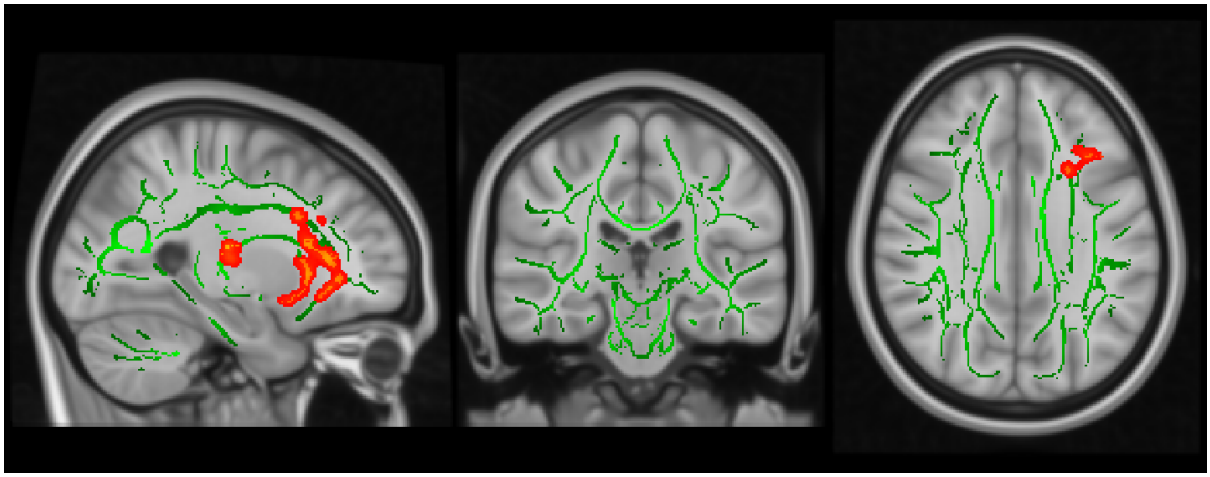

Figure S7. Exploratory dimensional TBSS analyses showing significant associations (red-yellow) between FA values and the CPRS scores over time. The mean FA skeleton across all subjects (green) was overlain on the MNI template image for presentation (x=-25, y=-25, z=31). Results were thickened for visualization (FSL "tbss_fill") and presented here in radiological convention from sagittal, coronal, and axial perspectives, respectively. A more negative change in FA (i.e. more isotropic diffusion) over time was associated with more HI symptom remission in ten clusters spread over six WM tracts. See Table S2 for cluster statistics and locations.